Adsorption kinetics and diffusion of Saxitoxins on granular-activated carbon: influence of pore size distribution

Neuma Maria Silva Buarque, Hugo Leonardo de Brito Buarque and Jose Capelo-Neto

ABSTRACT

Saxitoxin (STX) is the most toxic non-protein substance known. STX-producing cyanobacteria have been identified in most continents and are being detected more widely because of global warming, threatening human drinking water supplies worldwide. Removal of these components can be accomplished by adsorption on granular-activated carbon (GAC) but little is yet known about the kinetics of the process. This research investigated adsorption kinetics and diffusion behaviour of a decarbomoyl saxitoxin (dc-STX) and a carbamate toxin (STX) on four coconut shell-based GAC samples with different pore size distribution. It was observed that equilibrium concentration was reached within 24 h and that a pseudo-second-order model best represented experimental data. Of the four GAC samples tested, the example with the largest volume of mesopores adsorbed more STX and with a faster upload rate, while dc-STX was adsorbed equally in all four GAC samples.

Key words | adsorption kinetics and diffusion, granular-activated carbon, saxitoxins

Neuma Maria Silva Buarque
Water Company of Ceara (CAGECE) - Av. Dr. Lauro Vieira Chaves,
1030-Vila União, Fortaleza/CE,
Brazil. CEP: 60.420–280

Hugo Leonardo de Brito Buarque
Federal Institute of Education,
Science and Technology of Ceará – Av. Treze de Maio,
2081, Benfica – Fortaleza/CE,
Brazil. CEP 60.040–531

Jose Capelo-Neto (corresponding author)
Federal University of Ceara/SA Water, 40 Cheltenham St., Highgate, Adelaide, SA 5063, Australia
E-mail: *zecapelo@hotmail.com*; *capelo@ufc.br*

INTRODUCTION

Saxitoxins (STXs), also known as paralytic shellfish poisons (PSPs), have been associated with multiple human intoxications through seafood consumption, resulting in numbness, paralysis and death (Kuiper-Goodman *et al.* 1999). Besides poisoning by ingestion of food, humans may be exposed to cyanotoxins through the ingestion of contaminated drinking water and accidental ingestion, inhalation or dermal adsorption during recreational activities in waters affected by a toxic bloom (Merel *et al.* 2013). PSPs can be divided into three groups, the carbamates, the sulfamates and the decarbamoyl toxins (Figure 1 and Table 1). The molecular structure of STX has several amine groups that can gain protons and become cationic depending on the solution pH. As a result, up to 10 different species of STX exist (Hilal *et al.* 1995).

Paerl & Paul (2012) suggested that because of climate change, the frequency and intensity of harmful cyanobacteria blooms are expected to increase globally. These blooms can directly influence the quality of drinking water through the production of toxic metabolites. PSP-producing cyanobacteria have been increasingly reported in fresh and brackish water in many countries worldwide (Humpage *et al.* 1994; Kaas & Henriksen 2000; Sevcik *et al.* 2003; Liu *et al.* 2006; Ballot *et al.* 2010; Berry & Lind 2010; Clemente *et al.* 2010). According to Shi *et al.* (2012), the concentrations of extracellular STXs in these countries range up to 15 μg STX_{equiv} L^{-1} in natural waters, with intracellular gravimetric STXs concentrations ranging from 5 to 3,400 μg $STX_{equiv.}$ g^{-1} of cell dry weight.

Australia adopted a PSP health alert level of 3 μg $STX_{equiv.}$ L^{-1} for drinking water (NWQMS 2004), while a maximum PSP concentration of 1–3 μg $STX_{equiv.}$ L^{-1} is currently required by the New Zealand and Brazilian Ministry of Health, respectively (Orr *et al.* 2004; Portaria 2914 2011).

Because conventional water treatment plants (CWTPs) cannot remove extracellular cyanotoxins and other

doi: 10.2166/aqua.2015.140

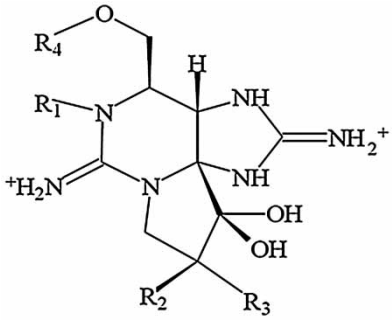

Figure 1 | Structural variations and characteristics of the STX class of cyanotoxins (Ho *et al.* 2009).

Table 1 | General structure, corresponding R functional groups, and relative toxicity for the most common PSP variants

	R1	R2	R3	Relative toxicity
R4 = $CONH_2$ (carbamate toxins)				
STX	H	H	H	1
Neo-STX	OH	H	H	0.924
GTX1	OH	H	OSO_3^-	0.994
GTX2	H	H	OSO_3^-	0.359
GTX3	H	OSO_3^-	H	0.638
GTX4	OH	OSO_3^-	H	0.726
R4 = $CONHSO_3^-$ (*N*-sulfocarbamoyl (sulfamate) toxins)				
C1	H	H	OSO_3^-	0.006
C2	H	OSO_3^-	H	0.096
R4 = H (decarbamoyl toxins)				
dc-STX	H	H	H	0.513
dc-neo-STX	OH	H	H	–
dc-GTX1	OH	H	OSO_3^-	–
dc-GTX2	H	H	OSO_3^-	0.651
dc-GTX3	H	OSO_3^-	H	0.754
dc-GTX4	OH	OSO_3^-	H	–

Source: Adapted from Ho *et al.* (2009).

metabolites, one of the last barriers available to prevent these substances from reaching households are granular-activated carbon (GAC) filters. However, there is no accurate way to predict how effectively a full-scale GAC filter will remove compounds such as STXs (Ho & Newcombe 2010). The equilibrium concentration of dissolved toxins is the maximum reduction level that can be achieved. However, a sufficient contact time has to be ensured to achieve equilibrium. Insufficient contact times may result in non-equilibrium conditions and reduce theoretical removal capacity. Therefore, adsorption kinetics is an important factor, particularly when working with slow adsorbing compounds (Fuerhacker *et al.* 2001).

Activated carbon surface charge and pore structure are important parameters for removal of organic compounds in water treatment (Li *et al.* 2002; Quinlivan *et al.* 2005; Zhang *et al.* 2010). Non-electrostatic interaction is the most common adsorption mechanism for apolar organic chemicals on activated carbon. On the other hand, organic compound with a cationic or anionic character may be poorly adsorbed via non-specific physisorption, while electrostatic mechanisms are enhanced (Shi *et al.* 2012). These authors showed that water pH has a large impact on the adsorptive efficiency of powdered-activated carbon (PAC) for STX removal, not only because it will determine STX charge, but also carbon surface charge.

Zhang *et al.* (2011) demonstrated that natural organic matter (NOM) may decrease removal of synthetic organic chemicals on activated carbon by competing for adsorption sites, and thereby reducing the surface area available, and by blockage or diffusional hindrance of pores. They also found that the minimum NOM hindrance effect occurred on the surface of the carbon dominated by mesopores, while severe NOM effects were observed primarily on the microporous carbons.

A few researchers have studied adsorption of STXs on activated carbons in aqueous solutions (Bailey *et al.* 1999; Newcombe & Nicholson 2002; Orr *et al.* 2004; Silva 2005; Ho *et al.* 2009; Shi *et al.* 2012). Shi *et al.* (2012) showed that STX can be effectively controlled at a common pre-disinfection pH of 8.2 with a PAC dose between 10 and 20 mg L^{-1}. Silva (2005) demonstrated that PAC presented high removals of neo-STX and STX, decreasing concentrations by as much as 28 μg L^{-1}. Orr *et al.* (2004) used GAC packed columns with an empty bed contact time of 15 min and removed 100% of decarbomoyl saxitoxin (dc-STX), STX, GTX-2/3 and GTX-5, 94% of dc-GTX-2/3, but only partially reduced *N*-sulfocarbamoyl-gonyautoxins 2 & 3: C1 & C2 toxins by 56% and 74%, respectively. Ho *et al.* (2009) developed experiments with PAC using two Australian raw waters. Happy Valley water had initial $STX_{equiv.}$ concentrations between 3.7 and 4.1 μg L^{-1} and Myponga between 7.5 and 9.9 μg L^{-1}. In both cases they were able to decrease

concentrations below 3.0 μg L^{-1} with a PAC dose of 10 mg L^{-1} (CT = 15 min) and 30 mg L^{-1} (CT = 70 min), respectively. These studies, however, neither presented appropriate kinetic modelling of adsorption data nor evaluated them in the context of carbon characterisation, especially pore size distribution (PSD) and surface charge, which makes it difficult to extend their findings to further GAC investigations or to real treatment situations. The hypothesis tested was PSD can effectively influence the amount and the rate of the removal of STX and dc-STX from water. Therefore, the aim of this study was to investigate the influence of PSDs in the adsorption of STX and dc-STX on four commercially available coconut shell GAC samples, all with a net positive surface charge, to determine the kinetic data and to provide elements for further modelling studies and real treatment design.

MATERIALS AND METHODS

STX production and semi-purification

The strain *Cylindrospermopsis raciborskii* T3–CR (Lagos *et al.* 1999) from the collection of the Federal University of Rio de Janeiro, Brazil, was used to produce STXs for the adsorption experiments. CR cultures were grown in ASM-1 medium (Gorham *et al.* 1964), with a pH of 8.0, under a white light intensity of 75 μ mol m^{-2} s^{-1}, at a temperature of 24 ± 2 °C, with aeration and a 12:12 light/dark photoperiod until they reached the end of the lag period. Although Carneiro *et al.* (2009) demonstrated that this strain can produce STX, neo-STX, dc-STX and dc-neo-STX, high performance liquid chromatography (HPLC) analysis demonstrated that our culture produced only STX and dc-STX in a sufficient amount to be used in the adsorption experiments.

To perform the extraction of intracellular STXs, the culture's biomass was concentrated by centrifugation at 2,700 G for 15 min (25 °C), the supernatant was discarded, and the pellets were collected. The pelleted material was subjected to three freeze–thaw cycles, filtered through a 0.45 μm nitrocellulose membrane (Macherey-Nagel, Bethlehem, PA, USA) and the filtrate was then subjected to a semi-purification step by solid phase extraction on C18 cartridges (Supelco, Bellefonte, PA, USA), according to Lawrence *et al.* (2005). The semi-purified extract was acidified with 0.1 M acetic acid (Merck, Darmstadt, Germany) to a pH of approximately 4.0 and stored at –20 °C to preserve STX stability (Indrasena & Gill 2000). It is important to note that this semi-purified extract contained not only dc-STX and STX, but other intracellular metabolites considered here as dissolved organic carbon (DOC). We believe that this approach more realistically represents the behaviour of the adsorption process since, in the case of an algal bloom, other dissolved intracellular compounds, apart from STXs, would be proportionally present in the water matrix and would not be removed by the CWTP.

Analytical methods

The semi-purified extract was characterised by analysing STX, dc-STX and DOC. DOC was measured with a total organic carbon analyser (Aurora 1030C, OI Analytical Co., Golden, CO, USA). STXs analysis were performed by HPLC using an Agilent 1260 equipped with a quaternary pump, a C18 chromatography column (250 × 4 mm, 5 μm) maintained at 30 °C, a manual injector with a loop of 20 μL, and a fluorescence detector–FLD with excitation of 340 nm and emission of 390 nm. As mobile phase, a 0.05 M ammonium formate aqueous solution with 5% HPLC grade acetonitrile (A) and a 0.1 M ammonium formate aqueous solution (B) with a total flow rate of 1.5 mL min^{-1} were applied. The process began with 100% mobile phase A. From 0 to 7.5 min, phase B increased from 0 to 20%. From 7.5 to 11 min, phase B increased from 20 to 80%, remaining unchanged until min 13. From 13 to 15 min it returned to 100% of A. The above methodology was adapted from Lawrence *et al.* (2005) and was validated (Silvino & Capelo-Neto 2014) using pre-column derivatisation method and STX standards from the Institute for Marine Bioscience (National Research Council–Halifax, Canada).

GAC sample characterisation

Coconut shell, an agricultural by-product from renewable resources, is the most abundant and affordable raw material used to produce activated carbon in Northeast Brazil (Jaguaribe *et al.* 2005) and therefore, was the focus of this

research. Four commercially available activated carbons produced with coconut shell using steam activation were used and named as GAC samples C1, C2, C3 and C4.

A porosimetry system (ASAP 2000, Micrometrics, Norcross, GA, USA) was used to measure N_2 (at 77 K) adsorption-desorption isotherm over a relative pressure (p/p_o) range of 10^{-6}–1. The surface area was calculated using the Brunauer–Emmett–Teller (BET) (Brunaer *et al.* 1938) equation and the total pore volume was estimated by converting the amount of adsorbed N_2 ($cm^3\ g^{-1}$ STP) to its liquid volume (Guo & Lua 2000). The PSD was obtained using density functional theory (Kowalczyk *et al.* 2003). The iodine number (mg of iodine adsorbed per g of carbon) was determined according to ASTM D 4607-86 (1994). The point of zero charge (PCZ) pH, i.e. the pH above which the total net surface of the carbon particles are negatively charged (Leon y Leon *et al.* 1992), was measured by the pH drift method (Newcombe *et al.* 1993).

Adsorption experiments

A batch system was applied to study the adsorption kinetics of STX and dc-STX in aqueous solution by GAC samples C1, C2, C3 and C4. Virgin GAC samples were wet sieved between Tyler Standard Mesh 60 (0.25 mm) and 65 (0.21 mm). Since these experiments were meant to simulate future short bed adsorber tests in a 20 mm internal diameter (ID) column, sieving the GAC sample to this diameter (particle diameter < 50 × column ID) was necessary in order to minimise channelling and wall effect in the column (Martin 1978). Each GAC sample was washed with 10 times its volume with ultrapure water to remove fine particles, then dried in a 110 °C oven to constant weight and cooled in a desiccator where it was stored prior to use (Summers *et al.* 1992). The water samples were prepared using ultrapure water, with an electrolyte concentration of 0.01 M NaCl, buffered with 10 mM phosphate to pH of 7.0 and spiked with semi-purified STX extract.

For the batch experiments, 3 mg of each GAC sample were placed in 12-mL amber glass vials along with 10 mL of water sample described previously. In each vial, the initial toxin concentrations (C_0) were 10.5 μg L^{-1} for dc-STX and 60.4 μg L^{-1} for STX. This can be considered a worst-case scenario for dissolved STXs in treated water. The DOC of the synthesised treated water spiked with STXs was 2.5 mg L^{-1}, between the range (1 and 5 mg L^{-1}) observed in real treated water (Internal report–CAGECE 2014). The vials were then quickly placed into a tumbler, and overturned continuously at 15 rpm, in the dark, and in a temperature controlled chamber at 28 °C. Individual vials were than collected hourly up to 8 h and then with less frequency until 48 h. A subsample of 2 mL was removed from the collected vial, filtered through a 0.45 μm syringe filter (Acrodisc, Pall Corp., Port Washington, NY, USA) and stored at –20 °C until analysis. HPLC analysis occurred 48 h after the first vial was collected. To observe if degradation or any other kind of removal besides carbon adsorption occurred, a control vial (without GAC sample) was submitted to the same conditions.

Adsorption modelling

Pseudo-first-order kinetic model (Equation (1)), also known as the Lagergren equation, was originally developed to describe adsorption of oxalic and malonic acids on carbons.

$$\log(q_e - q) = \log(q_e) - \frac{k_1 t}{2,303} \quad (1)$$

where q (μg mg^{-1}) is the amount of the component adsorbed in a given time t (min), q_e (μg mg^{-1}) is the amount adsorbed at equilibrium and, k_1 (min^{-1}) is the pseudo-first-order constant. q_e and k_1 can be calculated from the slope and intercept of the graph log ($q_e - q$) versus t. In published literature, it has been shown to effectively describe the absorption of drugs (Van Doorslaer *et al.* 2011), pesticides (Vulliet *et al.* 2002; Fresno *et al.* 2005) and dyes (Shen *et al.* 2012).

Ho & McKay (2000) developed the expression of pseudo-second-order rate (Equation (2)), which describes, generally, chemisorption involving valence forces by sharing or exchange of electrons between adsorbent and adsorbate

$$\frac{t}{q} = \frac{1}{k_2 q_e^2} + \frac{t}{q_e} \quad (2)$$

where k_2 (mg μg^{-1} min^{-1}) is the pseudo-second-order constant, q_e and q (μg mg^{-1}) are the amounts adsorbed at equilibrium and at a given time t, respectively. The constant

k_2 is determined by the slope of the graph of t/q versus t. Ho (2006) reported that the pseudo-second-order kinetics has been widely applied to the adsorption of pollutants on aqueous solutions.

Weber & Morris (1963) proposed the intraparticle diffusion model (Equation (3)) to evaluate the relevance of intraparticle diffusion in the adsorption process. In this model, if intraparticle diffusion is involved in adsorption, then a plot of the amount of adsorbate per unit mass of adsorbent (q) against square root of time ($t^{1/2}$) would be a straight line and, if this line crosses the origin, intraparticle diffusion is the limiting step.

$$q = k_{di}t^{1/2} + C \quad (3)$$

where k_{di} (mg μg^{-1} s$^{-1/2}$) is the intraparticle diffusion coefficient and C is the intercept. C expresses the magnitude of the boundary layer. The higher the value of C, the greater the effect of the boundary layer, that is, as values of C tends to zero, the boundary layer resistance should decrease its importance in the overall adsorption process.

The kinetic experimental data obtained were mathematically modelled with pseudo-first-order kinetics, pseudo-second-order kinetics, and intraparticle diffusion models. Linear regression was incorporated to judge the adequacy of the models. Statistical differences between GAC sample adsorption were tested using t-tests and chi-square. Significance was tested at the confidence level of $p_o = 0.05$.

RESULTS AND DISCUSSIONS

GAC sample characterisation

The net surface charges of GAC samples C1, C2, C3 and C4 were mainly positive at the working solution pH (7.0) since their pH_{PCZ} are 8.7, 8.8, 10 and 9.0, respectively. Examination of Table 2 shows that, except for C1, GAC samples have a high surface area and micropore volume. In terms of mesopores, GAC sample C3 has a relatively high volume (23%), indicative of an 'open' pore structure, while the other GAC samples only have a small volume of macropore and thus a much more 'closed' pore structure. The GAC samples used in this study therefore had the same surface charge but different surface areas and PSDs. Although Iodine number is reported in the literature to correlate well with micropore volume (Bacaoui *et al*. 2001; Nunes & Guerreiro 2011), no correlation was found between Iodine number and any other parameter evaluated (data not shown).

Kinetic modelling

The control sample showed that up to 48 h no significant degradation ($p_o = 0.05$) of toxins occurred. By adjusting the pseudo-first-order and pseudo-second-order models to the experimental data, it was possible to calculate k_1, k_2, q_{e1} and q_{e2} for the adsorption of dc-STX and STX (Table 3).

Table 2 | Characteristics of four coconut shell GAC samples used

GAC samples	C1		C2		C3		C4	
Raw material/activation method	Coconut shell/steam		Coconut shell/steam		Coconut shell/steam		Coconut shell/steam	
BET area (m^2 g^{-1})	487		981		1,001		1,018	
Total pore vol. (mL g^{-1})	0.215		0.446		0.494		0.525	
Micropore vol. (mL g^{-1}/%)	0.178	83%	0.381	85%	0.374	76%	0.437	83%
Mesopore vol. (mL g^{-1}/%)	0.024	11%	0.047	11%	0.114	23%	0.071	14%
Macropore vol. (mL g^{-1}/%)	0.013	6%	0.018	4%	0.006	1%	0.017	3%
Average pore size (nm)	1.126		1.813		1.971		2.060	
Iodine number (mL g^{-1})	397.5		739.4		454.7		662.3	
pH_{PCZ}	8.7		8.8		10.0		9.0	
Carbon charge at pH 7,0	+		+		+		+	
Average particle size (mm)	0.23		0.23		0.23		0.23	

Table 3 | Pseudo-first-order and pseudo-second-order kinetic constants and correlation coefficients

		Pseudo-first-order			Pseudo-second-order		
GAC sample	Toxin	q_{e1} (μg mg^{-1})	k_1 (min^{-1})	R^2	q_{e2} (μg mg^{-1})	k_2 (mg μg^{-1} min^{-1})	R^2
C1	dc-STX	0.050	0.046	0.711	0.035	8.690	0.974
	STX	0.124	0.013	0.777	0.143	1.604	0.968
C2	dc-STX	0.026	0.016	0.905	0.033	6.598	0.943
	STX	0.171	0.033	0.921	0.203	1.892	0.970
C3	dc-STX	0.027	0.013	0.418	0.032	17.412	0.979
	STX	0.127	0.010	0.464	0.252	3.034	0.982
C4	dc-STX	0.032	0.010	0.179	0.037	12.821	0.969
	STX	0.249	0.031	0.905	0.239	0.887	0.927

The correlation coefficients (R^2) of the pseudo-first-order kinetics were lower than the pseudo-second-order coefficients for adsorption of dc-STX and STX on all four GAC samples utilised, indicating that the adsorption process followed pseudo-second-order kinetics and that the rate-limiting step may be chemisorption. In addition, the calculated q_e for the pseudo-first-order kinetic showed a larger error compared to the experimental values, while for pseudo-second-order, the errors between calculated and experimental q_e varied by ± 9%.

GAC sample pore size distribution

GAC sample C3, with a greater amount of mesopores (23%), presented the largest STX adsorption capacity ($q_{e2} = 0.252$ μg mg^{-1}) although its BET area and pore volume were approximately the same as GAC samples C2 and C4 ($p_o = 0.05$). Ding (2010) performed experiments using PAC samples with different PSD to remove atrazine in different source waters containing NOM. The author found that the greater the volume of mesopores, the smaller the pore blockage by NOM and the larger amount of atrazine was adsorbed. Silva (2005) also found a relatively close relation between STXs adsorption capacity and mesoporous volume in PAC samples.

The maximum adsorption capacity of STX found in this study is still small compared to the one (0.625 μg L^{-1}) found by Shi *et al.* (2012). GAC sample C1 adsorbed the smallest amount of STX ($q_{e2} = 0.143$ μg mg^{-1}) probably due to its smaller BET area and average pore size compared to the other GAC samples tested. This same behaviour was not observed for dc-STX, which showed statistically ($p_o = 0.05$) the same adsorption capacity (q_{e2}) for all four GAC samples. Another point observed from Table 3 is that, except for GAC sample C1, the relation between q_{e2} for STX and q_{e2} for dc-STX was approximated ($p_o = 0.05$) to the initial STXs concentration ratio. This might indicate that there was no significant competitive advantage for occupation of adsorption sites between these two compounds on GAC samples C2, C3 and C4.

Pseudo-second-order constants (k_2) were greater for adsorption of dc-STX as compared to STX on all four GAC samples despite the initial concentration of dc-STX being lower than STX. It has to be noted, however, that dc-STX has a smaller molecular weight than STX. GAC sample C3, with the largest volume of mesopores, had the greater k_2 both for STX and dc-STX, suggesting that mesopore volume might influence not only the adsorption capacity, but also the rate in which those components are adsorbed.

Using the pseudo-second-order kinetic constants (Table 3) and the method utilised by Unuabonah *et al.* (2008), it was possible to generate fits for adsorption of

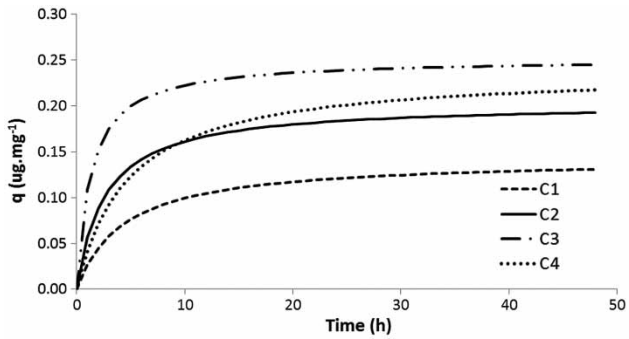

Figure 2 | Pseudo-second-order kinetic non-linear curves for adsorption of STX on C1, C2, C3 and C4 coconut shell GAC samples.

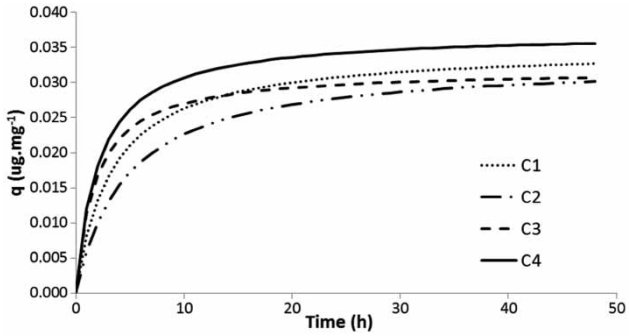

Figure 3 | Pseudo-second-order kinetic non-linear curves for adsorption of dc-STX on C1, C2, C3 and C4 coconut shell GAC samples.

STX (Figure 2) and dc-STX (Figure 3) using non-linear second-order kinetics equations. These results demonstrated that dc-STX and STX were slowly adsorbed. Although, 90% of the adsorbed concentrations occurred within 5–10 h, equilibrium concentrations were only reached within 24 h, corroborating with the equilibrium times for adsorption of STXs in PAC found by Silva (2005) and Shi *et al.* (2012).

Figure 4 shows the adsorption plots of q versus $t^{1/2}$ for dc-STX and STX on the GAC samples. Two different patterns can be observed in most graphs. Initially, there is a gradual adsorption stage where intraparticle diffusion has a greater or lesser influence in the adsorption process depending on the GAC sample and the STX involved, and after that, adsorption becomes very slow and approaches equilibrium. The relative influence of intraparticle diffusion resistance in the overall adsorption process decreases in this order in GAC samples C1 < C4 < C2 < C3 for STX and C1 < C2 < C4 < C3 for dc-STX, as intercept C increases (Table 4). As the GAC sample mesopore volume increases, the intercept C tends to move further way from the origin, indicating a decreasing influence of intraparticle diffusion and greater pore accessibility.

GAC sample surface charge

The molecular structure of dc-STX and STX have several amine groups that can potentially gain protons and, thereby, become cationic depending on the solution pH. At pH 7.1, Shi *et al.* (2012) observed that STX shifted to a mix of mono-cationic and di-cationic species (approximately 65% and 35%, respectively). This same behaviour can be extrapolated to dc-STX due to their molecular structure similarity. Owing to the cationic nature of the GAC sample surface and to the cationic speciation of dc-STX and STX, electrostatic repulsion appeared to be the dominant mechanism, explaining the small adsorption capacity encountered. In addition, as the solubility of dc-STX and STX increases and becomes more ionic, the hydrophobic driving force pushing STX from the aqueous phase is reduced concurrently, reducing the apparent adsorption capacity of the carbons.

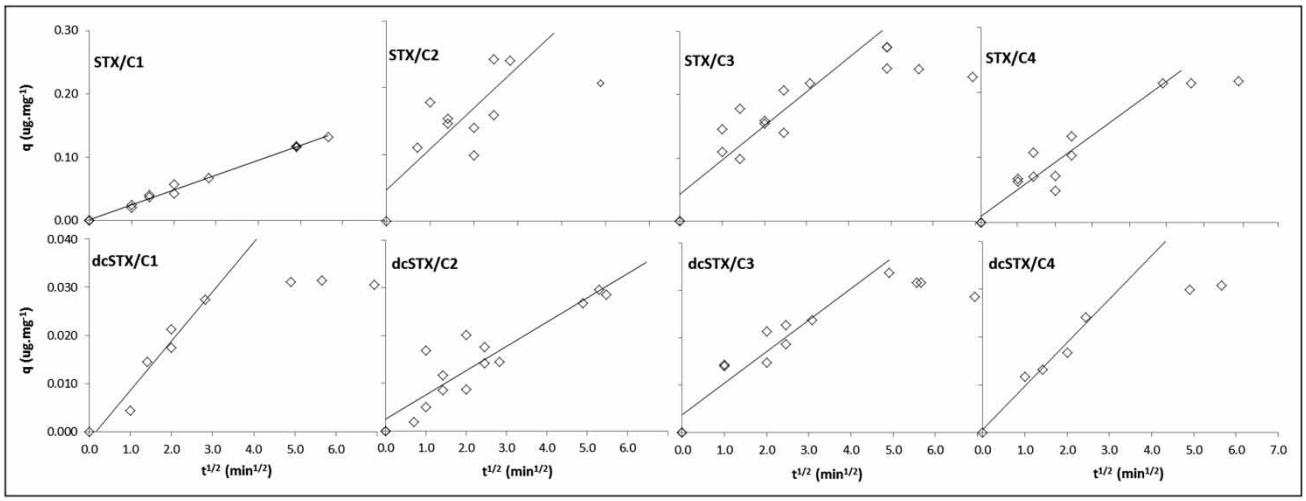

Figure 4 | Intraparticle diffusion model for adsorption of STX and dc-STX on GAC samples C1, C2, C3 and C4.

Table 4 | Intraparticle diffusion parameters for adsorption of STX and dc-STX on GAC samples

	STX			dc-STX		
GAC sample	k_p (mg g^{-1} h$^{-1/2}$)	C (mg g^{-1})	R^2	k_p (mg g^{-1} h$^{-1/2}$)	C (mg g^{-1})	R^2
C1	0,0233 ± 0,0005	0,0021 ± 0,0015	0,9978	0,0101 ± 0,0011	−0,0013 ± 0,0019	0,9674
C2	0,0653 ± 0,0185	0,0457 ± 0,0324	0,7132	0,0051 ± 0,0004	0,0020 ± 0,0013	0,9519
C3	0,0354 ± 0,0033	0,0913 ± 0,0091	0,9590	0,0047 ± 0,0003	0,0097 ± 0,0009	0,9819
C4	0,0414 ± 0,0058	0,0100 ± 0,0143	0,9282	0,0104 ± 0,0023	0,0036 ± 0,0037	0,8698

Bjelopavlic *et al.* (1999) showed that at pH 4 the NOM found in waters is negatively charged, and at pH 7 the magnitude of the negative charge is twice that at pH 4. It would be expected that for a positively charged activated carbon, there should be an attractive electrostatic interaction with NOM, while for the positively charged STXs, toxin–surface interaction should be repulsive. Therefore, it is viable to assume that besides the possible micropore blockage caused by high-molecular weight NOM, a favourable adsorption of NOM would further decrease adsorption capacity of dc-STX and STX, as suggested by Shi *et al.* 2012.

CONCLUSIONS

Kinetics of adsorption of dc-STX and STX on commercial coconut shell GAC samples followed a pseudo-second-order model, indicating that the rate-limiting step may be chemisorption. An equilibrium contact time of 24 h was identified for both dc-STX and STX, corroborating with results found in the literature. At the working solution pH (7.0) all four GAC samples presented a net positive surface charge which might have hindered adsorption of the positively charged STXs ($q_{e2} = 0.252$ μg mg^{-1} for STX and $q_{e2} = 0.037$ μg mg^{-1} for dc-STX on GAC sample C3). When compared to STX, dc-STX was poorly adsorbed, probably due to its smaller initial concentration, but had larger adsorption uptake rates for all GAC samples ($q_{e2} =$ 17.412 μg mg^{-1} for dc-STX and $q_{e2} = 3.034$ μg mg^{-1} for STX on GAC sample C3). The presence of NOM may have presented a strong competition for the adsorption sites, further decreasing STX removal. The low adsorption capacities displayed by the GAC samples may suggest that during the process of selecting an adsorbent for STX removal, a negatively charged activated carbon at the water pH would be preferred, as strongly supported in the literature. GAC sample C3, with the larger amount of mesopores, showed the largest adsorption capacity and uptake rate for STX indicating that, when comparing different GAC samples, PSD should be considered as important a parameter as BET area. The importance of PSD was also supported by the intraparticle diffusion model analysis, which displayed a relative decrease of intraparticle diffusion resistance in the overall adsorption process as mesopore volume increased. Finally, this study supports the idea that the selection of the activated carbon should be closely matched to the target component and to the treatment objectives.

ACKNOWLEDGEMENTS

We thank FINEP and CNPq for their financial support and CAGECE for kindly making available their staff, facilities, and important data to the development of this study. We also thank Rolando Fabris (SA Water) for his proof reading and important contributions.

REFERENCES

ASTM D 4607-86 1994 *Standard Test Method for Determining of Iodine Number of Activated Carbon*. Annual Book of ASTM Standards, Philadelphia, PA, pp. 5.01.

Bacaoui, A., Yaacoubi, A., Dahbi, A., Bennouna, C., Luu, R. P. T., Maldonado-Hodar, F. J., Rivera-Utrilla, J. & Moreno-Castilla, C. 2001 Optimization of conditions for the preparation of activated carbons from olive-waste cakes. *Carbon* **39** (3), 425–432.

Bailey, D., Bowen, B., Goodwin, L. & Procter, L. 1999 An organic removal strategy for Grahamstown WTP. In: *Proceedings Australian Water and Wastewater Association*, Adelaide, Australia, April 11–14.

Ballot, A., Fastner, J. & Wiedner, C. 2010 Paralytic shellfish poisoning toxin-producing cyanobacterium *Aphanizomenon gracile* in Northeast Germany. *Appl. Environ. Microbiol.* **76**, 1173–1180.

Berry, J. P. & Lind, O. 2010 First evidence of paralytic shellfish toxins and cylindrospermopsin in a Mexican freshwater system, Lago Catemaco, and apparent bioaccumulation of the toxins in tegogolo snails (*Pomacea patula catemacensis*). *Toxicon* **55**, 930–938.

Bjelopavlic, M., Newcombe, G. & Hayes, R. 1999 Adsorption of NOM onto activated carbon: effect of surface charge, ionic strength, and pore volume distribution. *J. Colloid Interface Sci.* **210**, 271–280.

Brunauer, S., Emmett, P. H. & Teller, E. 1938 Adsorption of gases in multimolecular layers. *J. Am. Chem. Soc.* **60**, 309–319.

Carneiro, R. L., Santos, M. E. V., Pacheco, A. B. F. & Azevedo, S. M. F. O. 2009 Effects of light intensity and light quality on growth and circadian rhythm of saxitoxins production in *Cylindrospermopsis raciborskii* (Cyanobacteria). *J. Plankton Res.* **1** (1), 1–8.

Clemente, Z., Busato, R. H., Oliveira Ribeiro, C. A., Cestari, M. M., Ramsdorf, W. A., Magalhães, V. F., Wosiack, A. C. & Silva de Assis, H. C. 2010 Analyses of paralytic shellfish toxins and biomarkers in a southern Brazilian reservoir. *Toxicon* **55**, 396–406.

Ding, L. 2010 Mechanisms of competitive adsorption between trace organic contaminants and natural organic matter on activated carbon. PhD Thesis. University of Illinois, Illinois, USA, p. 185.

Fresno, F., Guillard, C., Coronado, J., Chovelon, J. M., Tudela, D., Soria, J. & Herrman, J. 2005 Photocatalytic degradation of a sulfonylurea herbicide over pure and doped TiO_2 photocatalysis. *J. Photochem. Photobiol. A Chem.* **173**, 13–20.

Fuerhacker, M., Durauer, A. & Jungbauer, A. 2001 Adsorption isotherms of 17 β-estradiol on granular activated carbon (GAC). *Chemosphere* **44**, 1573–1579.

Gorham, P. R., Maclachlav, J. R., Hammer, V. T. & Kim, W. K. 1964 Isolation and culture of toxic srains of *Anabaena flos-aquae* (Lyngb.) de Bréb. *Verh. Int. Verein. Theoret. Angew. Limnol.* **15**, 796–804.

Guo, J. & Lua, A. C. 2000 Preparation of activated carbons from oil-palm-stone chars by microwave-induced carbon dioxide activation. *Carbon* **38** (14), 1985–1993.

Hilal, S., Karickhoff, S. W. & Carreira, L. A. 1995 A rigorous test for SPARC's chemical reactivity models: estimation of more than 4300 ionization pK_a's. *Quant. Struct. Activity Relationships* **14**, 348–355.

Ho, Y. S. 2006 Review of second order models for adsorption systems. *J. Hazard. Mater. B* **136**, 681–689.

Ho, H. S. & McKay, G. 2000 The kinetics of sorption of divalent metal ions onto Sphagnum moss peat. *Water Res.* **34**, 735–742.

Ho, L. & Newcombe, G. 2010 Granular activated carbon adsorption of 2-methylisoborneol (MIB): pilot- and laboratory-scale evaluations. *J. Environ. Eng.* **9**, 965–974.

Ho, L., Tanis-Plant, P., Kayal, N., Slyman, N. & Newcombe, G. 2009 Optimizing water treatment practices for the removal of *Anabaena circinalis* and its associated metabolites, geosmin and saxitoxins. *J. Water Health* **7**, 544–556.

Humpage, A. R., Rositano, J., Bretag, A. H., Brown, R., Baker, P. D., Nicholson, B. C. & Steffensen, D. A. 1994 Paralytic shellfish poisons from Australian cyanobacterial blooms. *Aus. J. Marine Freshwater Res.* **45**, 761–771.

Indrasena, W. M. & Gill, T. A. 2000 Thermal degradation of partially purified paralytic shellfish poison toxins at different times, temperatures, and pH. *J. Food Sci.* **65** (6), 948–953.

Jaguaribe, E. F., Medeiros, L. L., Barreto, M. C. S. & Araujo, L. P. 2005 The performance of activated carbons from sugarcane bagasse, babassu, and coconut shells in removing residual chlorine. *Brazil. J. Chem. Eng.* **22** (1), 41–47.

Kaas, H. & Henriksen, P. 2000 Saxitoxins (PSP toxins) in Danish lakes. *Water Res.* **34**, 2089–2097.

Kowalczyk, P., Terzyk, A. P. & Gauden, P. A. 2003 Estimation of the pore-size distribution function from the nitrogen adsorption isotherm. Comparison of density functional theory and the method of Do and co-workers. *Carbon* **41** (6), 1113–1125.

Kuiper-Goodman, T., Falconer, I. & Fitzgerald, J. 1999 In: *Toxic Cyanobacteria in Water: a Guide to Their Public Health Consequences, Monitoring and Management* (I. Chorus & J. Bartram, eds). E & F. N. Spon, London, pp. 113–153.

Lagos, L., Onodera, H., Zagatto, P. A., Andrinolo, D., Azevedo, S. M. F. O. & Oshima, Y. 1999 The first evidence of paralytic shellfish toxins in the freshwater cyanobacterium *Cylindrospermopsis raciborskii*, isolated from Brazil. *Toxicon* **37**, 1359–1373.

Lawrence, J. F., Niedzwiadek, B. & Menard, C. 2005 Quantitative determination of paralytic shellfish poisoning toxins in shellfish using pre-chromatographic oxidation and liquid chromatography with fluorescence detection: collaborative study. *J. AOAC Int.* **88** (6), 1714–1719.

Leon y Leon, C. A., Solar, J. M., Calemma, V. & Radovic, L. R. 1992 Evidence for the protonation of basal plane sites on carbon. *Carbon* **30**, 797.

Li, Q., Snoeyink, V., Campos, C. & Marinas, B. 2002 Displacement effect of NOM on atrazine adsorption by PACs with different pore size distributions. *Environ. Sci. Technol.* **36**, 1510–1515.

Liu, Y., Chen, W., Li, D., Shen, Y., Li, G. & Liu, Y. 2006 First report of aphantoxins in China – waterblooms of toxigenic *Aphanizomenon flos-aquae* in Lake Dianchi. *Ecotoxicol. Environ. Safety* **65**, 84–92.

Martin, H. 1978 Low peclet number particle-to-fluid heat and mass transfer in peaked beds. *Chem. Eng. Sci.* **33**, 913–925.

Merel, S., Walker, D., Chicana, R., Snyder, S., Baurès, E. & Thomas, O. 2013 State of knowledge and concerns on cyanobacterial blooms and cyanotoxins. *Environ. Int.* **59**, 303–327.

Newcombe, G. & Nicholson, B. 2002 Treatment options for the saxitoxin class of cyanotoxins. *Water Sci. Technol. Water Supply* **2** (5–6), 271–275.

Newcombe, G., Hayes, R. & Drikas, M. 1993 Granular activated carbon: importance of surface properties in the adsorption of naturally-occurring organics. *Colloid. Surf.* **78**, 65–71.

Nunes, C. A. & Guerreiro, M. C. 2011 Estimation of surface area and pore volume of activated carbons by methylene blue and iodine numbers. *Quim. Nova.* **34** (3), 472–476.

NWQMS–National Water Quality Management Strategy 2004 Australian Drinking Water Guidelines 6. Endorsed by National Health and Medical Research Council–NHMRC. Available from: www.nhmrc.gov.au/_files_nhmrc/publications/attachments/eh34_adwg_11_06.pdf (accessed 9 December 2014).

Orr, P. T., Jones, G. J. & Hamilton, G. R. 2004 Removal of saxitoxins from drinking water by granular activated carbon, ozone and hydrogen peroxide-implications for compliance with the Australian drinking water guidelines. *Water Res.* **38**, 4455–4461.

Paerl, H. W. & Paul, V. J. 2012 Climate change: links to global expansion of harmful cyanobacteria. *Water Res.* **46** (5), 1349–1363.

Portaria 2914 de 12, December of 2011 Brasília. Ministry of Health, Brazil.

Quinlivan, P., Li, L. & Knappe, D. 2005 Effects of activated carbon characteristics on the simultaneous adsorption of aqueous organic micropollutants and natural organic micropollutants and natural organic matter. *Water Res.* **39**, 1663–1673.

Sevcik, C., Noriega, J. & D'Suze, G. 2003 Identification of *Enterobacter* bacteria as saxitoxin producers in cattle's rumen and surface water from Venezuelan Savannahs. *Toxicon* **42**, 359–366.

Shen, C., Wang, Y. J., Xu, J. H. & Luo, G. S. 2012 Facile synthesis and photocatalytic properties of TiO_2 nanoparticles supported on porous glass beads. *Chem. Eng. J.* **209**, 478–485.

Shi, H., Ding, J., Timmons, T. & Adams, C. 2012 Ph effects on the adsorption of saxitoxin by powdered activated carbon. *Harmful Algae* **19** (64), 61–67.

Silva, A. S. 2005 Assessment of the ability of removal of saxitoxins by different types of powdered activated carbon (PAC) produced in Brazil. PhD Dissertation, UNB, DF, 115.

Silvino, L. S. & Capelo-Neto, J. 2014 Validation of analytical method for saxitoxin detection (STX and dc-STX) by high performance liquid chromatography with fluorescence detector and pre-column derivation. *Revista AIDIS* **7** (3), 243–258.

Summers, R. S., Cummings, L., DeMarco, J., Hartman, D. J., Metz, D. H., Howe, E. W., MacLeod, J. M. B. & Simpson, M. 1992 *Standardized protocol for the evaluation of GAC*. Report prepared for AWWA Research Foundation. American Water Works Association (AWWA), Denver.

Unuabonah, E. I., Adebowale, K. O. & Dawodu, F. A. 2008 Equilibrium, kinetic and sorber design studies on the adsorption of Aniline blue dye by sodium tetraborate modified Kaolinite clay adsorbent. *J. Hazard. Mater.* **157**, 397–409.

Van Doorslaer, X., Demeestere, K., Heynderickx, P. M., Van Langenhove, H. & Dewulf, J. 2011 UV-A and UV-C induced photolytic and photocatalytic degradation of ciprofloxacin and moxofloxacin: Reaction kinetics and role of adsorption. *Appl. Catalysis B Environ.* **101**, 540–547.

Vulliet, E., Emmelin, C., Chovelon, J., Guillard, C. & Herrmann, J. 2002 Photocatalytic degradation of sulfonylurea herbicides in aqueous TiO_2. *Appl. Catalysis B Environ.* **38**, 127–137.

Weber, W. J. & Morris, J. C. 1963 Kinetics of adsorption on carbon from solution. *J. Sanitary Eng. Div.* **89** (6), 53–55.

Zhang, S., Shao, T., Kose, H. & Karanfil, T. 2010 Adsorption of aromatic compounds by carbonaceous adsorbents: a comparative study on granular activated carbon, activated carbon fiber, and carbon nanotubes. *Environ. Sci. Technol.* **44**, 6377–6383.

Zhang, S., Shao, T. & Karanfil, T. 2011 The effects of dissolved natural organic matter on the adsorption of synthetic organic chemicals by activated carbons and carbon nanotubes. *Water Res.* **45**, 1378–1386.

First received 29 October 2014; accepted in revised form 15 December 2014. Available online 31 January 2015